Chemico-Biological Interactions 401 (2024) 111186

Contents lists available at ScienceDirect

Chemico-Biological Interactions

journal homepage: www.elsevier.com/locate/chembioint

Research paper

Molecular and toxicological mechanisms behind the effects of chromium (VI) on the male reproductive system of Mytilus galloprovincialis: First evidence for poly-ADP-ribosylation of protamine-like II

Carmela Marinaro [a,1], Alberto Marino [a,1], Anna Rita Bianchi [a,1], Bruno Berman [a], Marco Trifuoggi [b], Alessandra Marano [b], Giancarlo Palumbo [c], Teresa Chianese [a], Rosaria Scudiero [a], Luigi Rosati [a,d,2], Anna De Maio [a,***,2], Gennaro Lettieri [a,**,2], Marina Piscopo [a,*,2]

[a] Department of Biology, University of Naples Federico II, Via Cinthia, 21, 80126, Naples, Italy
[b] Department of Chemical Sciences, University of Naples Federico II, 21,80126, Naples, Italy
[c] Commodity Science Laboratory, Department of Economics, Management and Institutions, University of Naples Federico II, 80126, Naples, Italy
[d] CIRAM, Centro Interdipartimentale di Ricerca "Ambiente", University Federico II, Via Mezzocannone 16, 80134, Napoli, Italy

ARTICLE INFO

Keywords:
Chromium (VI)
poly(ADPribosyl)ation
Protamine-like proteins

ABSTRACT

Studies on the molecular mechanisms of heavy metal toxicity in invertebrate reproduction are limited. Given that PARP-catalysed ADP-ribosylation is also involved in counteracting heavy metal toxicity and maintaining genomic integrity, and that PARylation is implicated in chromatin remodelling but its role in sperm chromatin remains to be elucidated, we investigated the effects of chromium(VI) at 1, 10 and 100 nM on the reproductive health of *Mytilus galloprovincialis*. The damage to the gonads was assessed by morphological analyses and the damage indices PARP and ɣH2A.X were measured. Changes in the binding of protamine-like (PL) to DNA and the possibility of poly(ADP-ribosyl)ation of PL proteins were also investigated. Gonadal chromium accumulation and morphological damage were found, especially when the mussels were exposed to the highest dose of chromium (VI). In addition, the maximum expression of gonadal ɣH2A.X and PARP were obtained at 100 and 10 nM Cr(VI), respectively. Interestingly, for the first time in all exposed conditions, poly(ADP)-ribosylation was detected on PL-II, which, together with PL-III and PL-IV, are the major nuclear basic proteins of *Mytilus galloprovincialis* sperm chromatin. Since PL-II is involved in the final high level of sperm chromatin compaction, this post-translational modification altered the binding of the PL protein to DNA, favouring the action of micrococcal nuclease on sperm chromatin. This study provides new insights into the effects of chromium(VI) on *Mytilus galloprovincialis* reproductive system and proposes a molecular mechanism hypothesis describing the toxic effects of this metal on PL-DNA binding, sperm chromatin and gonads.

1. Introduction

It is well known that in response to genomic material damage, an increase of poly(ADP-ribose) polymerase 1 and 2 (PARP-1 and PARP-2) activities occurs. The two nuclear proteins PARP-1 and PARP-2 function as DNA nick-sensor enzymes and PARPs activation seems to be a crucial event for resisting heavy metals cytotoxicity and maintaining genomic integrity [1]. These enzymes can also be considered as new pollution biomarkers, because significant PARP activity variations were measured in both plants [2,3] and animals [4–8] exposed to xenobiotic agents. Upon binding to DNA breaks, PARPs work by using NAD^+ as their substrate to form branched poly(ADP-ribose) (PAR), which bind on

* Corresponding author.
** Corresponding author.
*** Corresponding author. Department of Biology, University of Naples Federico II, Via Cinthia, 21, 80126, Naples, Italy.
E-mail addresses: andemaio@unina.it (A. De Maio), gennarole@outlook.com (G. Lettieri), marina.piscopo@unina.it (M. Piscopo).
[1] These authors contributed equally to this work and are co-first.
[2] These authors are co-last.

https://doi.org/10.1016/j.cbi.2024.111186
Received 12 July 2024; Received in revised form 30 July 2024; Accepted 4 August 2024
Available online 6 August 2024

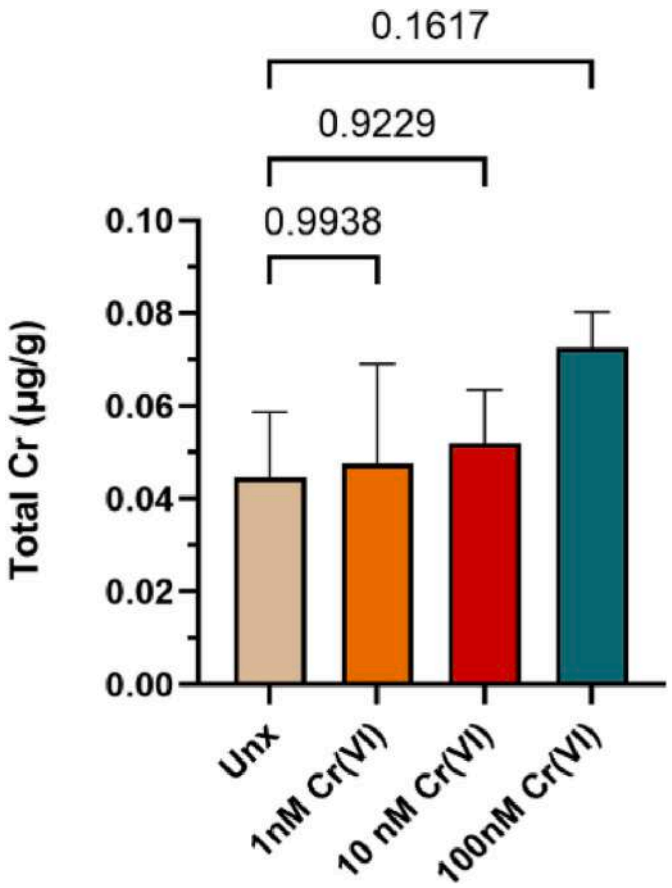

Fig. 1. The accumulation of total chromium in the male gonads of mussels after 24h of exposure to the indicated Cr(VI) concentration, compared to the unexposed control (Unx). The histograms show values as mean ± S.D.

target proteins and themselves [9]. PAR is known to mediate the response to damaged DNA and to control the organisation of chromatin, as well as the repair of DNA and the regulation of transcription [10]. Activation of PARP1 following DNA damage involves not only PARP1 auto-PARylation, as well as extensive PARylation of proteins found in chromatin, like histones [11,12] which is involved in the relaxation of the chromatin. Chromatin relaxation by poly(ADPribosyl)ation represents one of the mechanisms by which nuclear events, including DNA repair, are facilitated [13]. This because, the induction of DNA repair leads to increased levels of poly (ADP-ribose) polymerase activity, which determines nucleosome disassembly [14–16]. H1 histone was reported to be a covalent acceptors of PAR [17] and this modification occurs mainly on arginine, glutamate and lysine residues [18,19]. In addition, a non-covalent interaction was also demonstrated between histone linker H1 and PAR [20]. Several studies referred that core histones also are covalently and non-covalently modified with PAR [15,19,21,22]. *Mytilus galloprovincialis* (*M. galloprovincialis*) is a filter-feeding sessile organism that is able to accumulate many different types of contaminants in its tissues; it is a useful bioindicator in monitoring programs [23–26]. Chromium is an extremely toxic element, especially in its hexavalent form (Cr(VI)) [27–31]. Chromium and its compounds are extremely widespread, because of their vast use in industry [32]. For these reasons this metal is often present in the air, in rocks, in the soil, in ground water and even in organisms. Despite the fact that the concentration of chromium in seawater is less than 0.5 µg/L, the concentration of Cr(VI) in coastal groundwater that is contaminated by Cr-containing rocks or minerals and/or anthropogenic activities, combined with the inflow of seawater, can range up to hundreds of µg/L [33]. Variations in the chromium concentration in seawater have generated a vivid interest in the scientific community over the last 40 years [34–37]. Very little is well established about the effects of Cr(VI) on reproductive health of aquatic organisms. Generally, papers focused on fertilizating rates in organisms such as sea urchin and starfish [38] after very high doses of chromium exposure [39,39,40]. Even studies conducted with sub-lethal doses of Cr (8 ppm) have focused solely on alterations in indices of oxidative stress and sperm morphology [41]. In externally fertilized marine organisms, however, it is also useful the assessment of the impact of heavy metals on the components of sperm chromatin in consideration of their usefulness as a relevant biological target for assessing the genotoxicity of contaminants, thus making sperm chromatin a promising target for new strategies for rapid and sensitive toxicity assessment [42–45]. Chromium (VI) indeed is a toxic metal, carcinogenic, Reactive Oxygen Species (ROS) inducer and consequently genotoxic to DNA [46,47]. The major protein components of *M. galloprovincialis* sperm chromatin is the three protamine-like (PL) proteins named PL-II, PL-III and PL-IV [48]. PL proteins are part of the sperm nuclear basic proteins (SNBP), which bind to DNA in the sperm nucleus at the conclusion of the spermiogenesis process, and represent an intermediate group of proteins in terms of structure and function between the histones (H) and protamines (P) [49]. PL are histone-H1 related and are rich in both arginine and lysine [50,51]. First identified in bivalve molluscs, they have since been documented in the echinoderms, the tunicates and the vertebrates [52]. PL proteins in *M. galloprovincialis* account for 76 % of all sperm nuclear basic proteins (SNBP) of spermatozoa, divided into PL-II (20 %), PL-III (50 %) and PL-IV (6 %).These proteins are co-existent with 4 % of non-histone proteins and 20 % of somatic histones [37]. The *M. galloprovincialis* PL-II protein belongs to the H1 family of histones and possesses a conserved 84-residue globular core, closely analogous to the two histone H1 wing-helix motifs. PL-IV is a small protein and its composition is similar to that of the C-terminal tail of histone H1, which is rich in lysine [53]. In fact, PL-IV is the posttranslational cleavage product of a PL-II/PL-IV precursor [54]. PL-III, rich in lysine (27.5 mol/mol) and arginine (22.5 mol/mol), is a protein intermediate type among histones and protamines, but does not possess a typical secondary structure as protamines do in vitro [55]. It has never been investigated in the literature whether exposure of *M. galloprovincialis* to chromium can induce poly(ADP ribosyl)ation of PL proteins and its potential role in damage at multiple cellular levels. To address this gap in this study, *M. galloprovincialis* was treated with 1, 10 and 100 nM Cr (VI) and the chromium accumulated in the male gonad of mussels exposed was measured. Moreover, a morphological analysis of mussel gonad was conducted, and epigenetic alterations were determined. In detail, gonadal H2A.X phosphorylated (γH2A.X) and PARP expression and activity determinations were carried out, to verify possible oxidative DNA damages. Furthermore, for the first time, it was investigated a possible poly(ADPribosyl)ation of PL proteins, to verify whether and how their heteromodification could influence chromatin structure. Therefore, any changes in binding PL-DNA were assessed by Micrococcal nuclease (MNase) timed digestion and PL release from sperm nuclei. All findings were used to formulate a hypothesized molecular mechanism that describes the toxic effects of Cr(VI) on PL-DNA binding, sperm chromatin and gonads.

2. Materials and Methods

2.1. Reagents

The chemicals used for this study are of analytical grade. Unless otherwise specified, the chemical reagents were obtained from Merck (Rome, Italy).

2.2. Ethics statement

The model organism used in this study, *M. galloprovincialis* is not protected by any Italian environmental authority. The study was

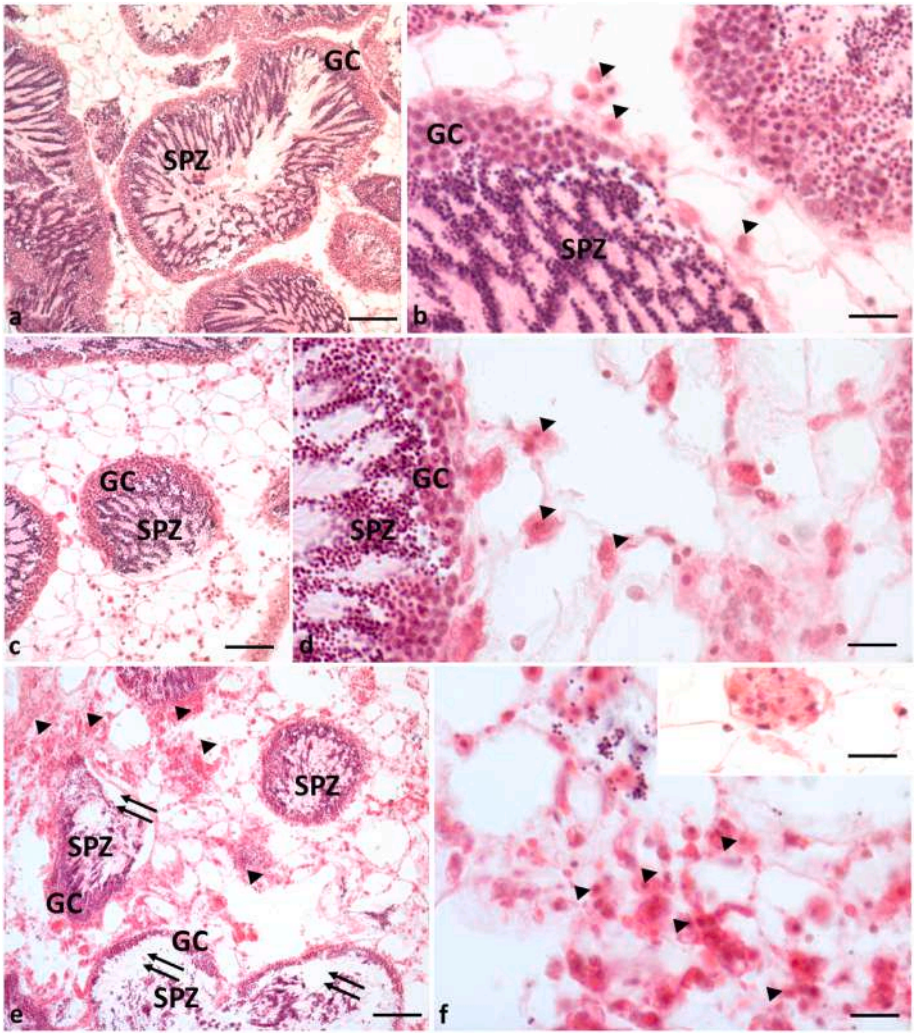

Fig. 2. Hematoxylin-Eosin staining (HE) of. M. galloprovincialis testis (a) Unexposed (Unx) animals; (b) animals exposed to 1 nM Cr; (c–d) animals exposed to 10 nM Cr; (e–f) animals exposed to 100 nM Cr. The insert (f) shows nodular formation of immune cells. Arrowhead: haemolymph immune-functioning cells present in the testis connective tissue of all treated animals. Double arrow: disconnection of the germ cells from each other and between the germ cells and the wall of the spermatic follicles. GC: germ cells at an early stage of differentiation. SPZ: Spermatozoa. Scale bars: a, c, e: 40 μm; b, d, f, insert f: 15 μm.

conducted in compliance with the treatment and use of animals for scientific purposes, according to the European (Directive 2010/63) and Italian (Legislative Decree No. 116/1992) directives.

2.3. Mussels sampling and chromium exposure

The conditions of exposure were performed following the protocols described in Piscopo et al., 2016 [56], and unexposed condition was prepared following the protocol described in Lettieri et al. (2019) [57]. Mussels were supplied by Eurofish Napoli S.R.L. Bacoli. These chromium doses are comparable to those found in the Mediterranean Sea [58].

2.4. Spermatozoa sampling and processing

Following 24 h of exposure, a knife was then used to open the mussels. Care was taken not to damage the soft tissue. The gonads were incubated for 5 min at 16 °C in 500 μL ASW to promote the release of gametes. The gametes were examined under a microscope at 40x magnification to identify the sex. After sex determination, some male gonads were used for chromium accumulation measurements. The ASW containing spermatozoa was first centrifuged at 2000×*g* for 2 min to remove debris, and after centrifuging at 9000×*g* for 10 min the supernatants spermatozoa were collected. Pellets of spermatozoa and male gonads were stored at −80 °C.

2.5. Chromium determination in gonads

For the ICP-MS evaluations, high purity water (resistivity of 18.2 MΩ cm) was taken from a Milli-Q unit (Millipore, USA). This was used to prepare the standards and to dilute the samples. Nitric acid (HNO_3, 69 % v/v Ultratrace@ ppb-trace analysis grade) was provided by Scharlau (Barcelona, Spain). A certified reference solution containing Cr at 100 mg/L of ultrapure grade for ICP, VWR Avantor® (Pennsylvania, US) was used.

Cr was determined by inductively coupled plasma mass spectrometry (ICP-MS Aurora M90, Bruker, Germany) in normal sensitivity mode. The calibration curve for the quantification of Cr ranged from 0.1 to 100 μg/L and was established daily by analysing standard solutions prepared immediately before the analysis. HNO_3 solution (2 %, v/v) was used for all standards used in the analysis. In both the calibration curve and the sample analysis, the internal standards were 89Y and 115In. With an R2 value greater than 0.9996, the linearity was acceptable. The treatment of samples involved a wet digestion: gonads were wet digested with 1 ml of ultrapure HNO_3 (67–69 %, v/v). The mixture was gently boiled for 3 h at 90 °C to obtain a clear solution. After cooling, a solution of HNO3 (2 %, v/v) was added to a final volume of 10 mL. The solutions obtained

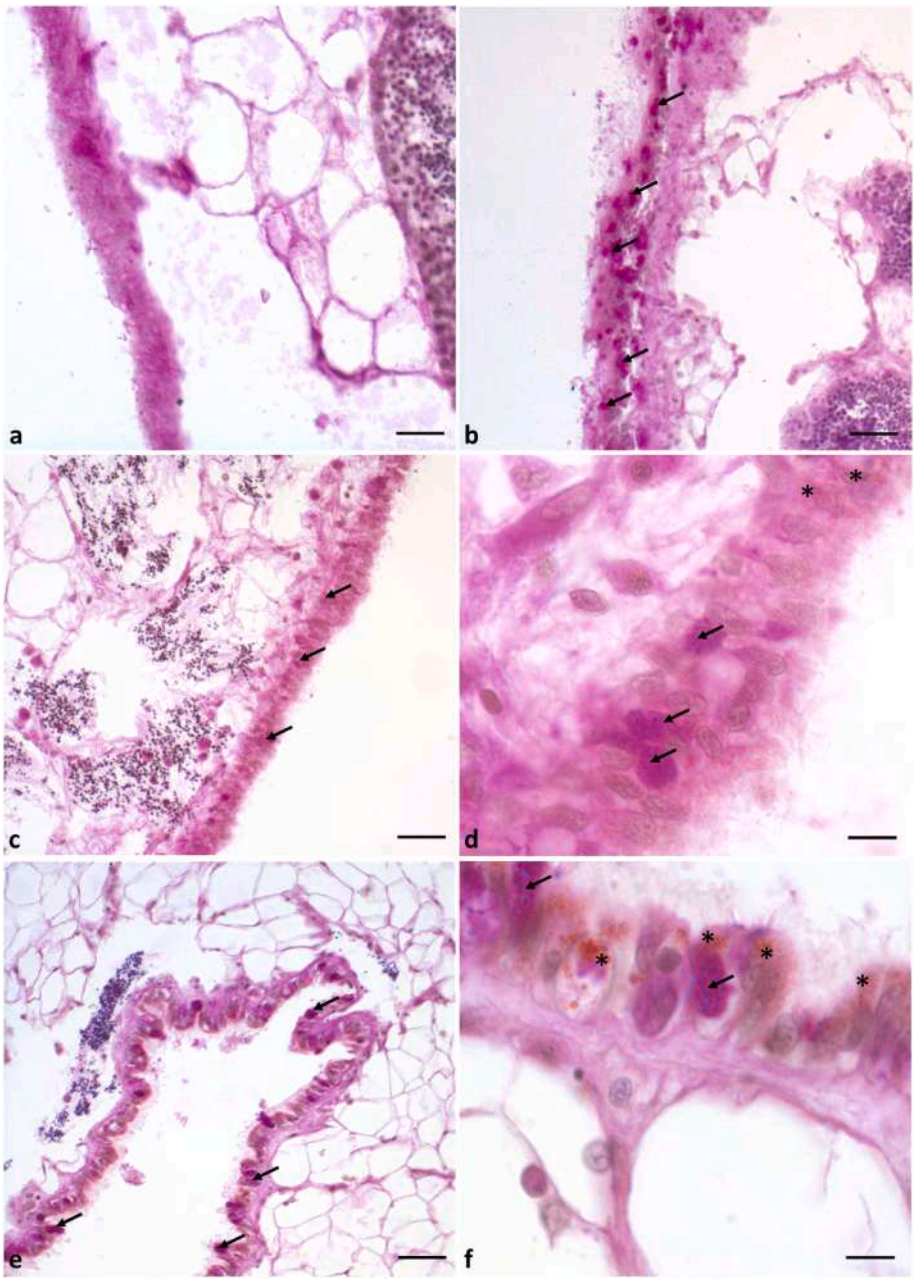

Fig. 3. Testis of M. galloprovincialis PAS stained. (a) Unexposed animals (Unx); (b) Exposed with 1 nM Cr; (c–d) Exposed with 10 nM Cr; (e–f) Exposed with 100 nM Cr. Hypertrophic and hyperplastic goblet cells (arrow) distributed in the peripheral connective tissue are present in the testes of all exposed mussels. Asterisk: lipofuscin granules. Scale bars: a,b: 20 μm; c,e: 30 μm; d,f: 10 μm.

were analysed by ICP-MS.

2.6. Histological analyses

The organization and morphology of the testes of unexposed and exposed mussels to the contaminant were studied by fixing the tissues in Bouin's solution, dehydrated in graded alcohols (first 75 %, then 96 % and finally 3 steps at 100 %), cleared with xylene and embedded in paraffin. Serial sections of 6 μm were mounted on glass slides and processed for routine histological analysis as Hematoxylin-Eosin (HE) and Periodic Acid-Schiff (PAS) staining as described previously [59]. Briefly, for HE analysis, slides were initially stained with 0.25 % eosin acidified with acetic acid (to stain the cytoplasm in pink), and nuclei were subsequently stained blue with 1 % Mayer's hemallumen. With the PAS reaction, histological material was first treated with periodic acid that oxidizes the 1,2-glycol groups to aldehydic groups, then, by adding the Schiff's reagent in the second step, the aldehydes took on a magenta-red colour. As a result, the PAS reaction produced specific staining for unsubstituted polysaccharides, neutral mucopolysaccharides, mucus and glycoproteins. All morphology observations were made with the Zeiss Axioskop microscope and images were taken with Axiovision 4.7 software (Zeiss) [60].

2.7. Extraction of PL proteins from M. galloprovincialis spermatozoa

Extraction of PL from unexposed and exposed mussel to Cr(VI), was conducted by using perchloric acid as described in Lettieri et al., 2021 [61]. For this study, n = 2 male gonads were used from each tank. Each gonad was used for one exposure condition. The gonads were homogenized and acid extraction was performed as described by Notariale et al.,

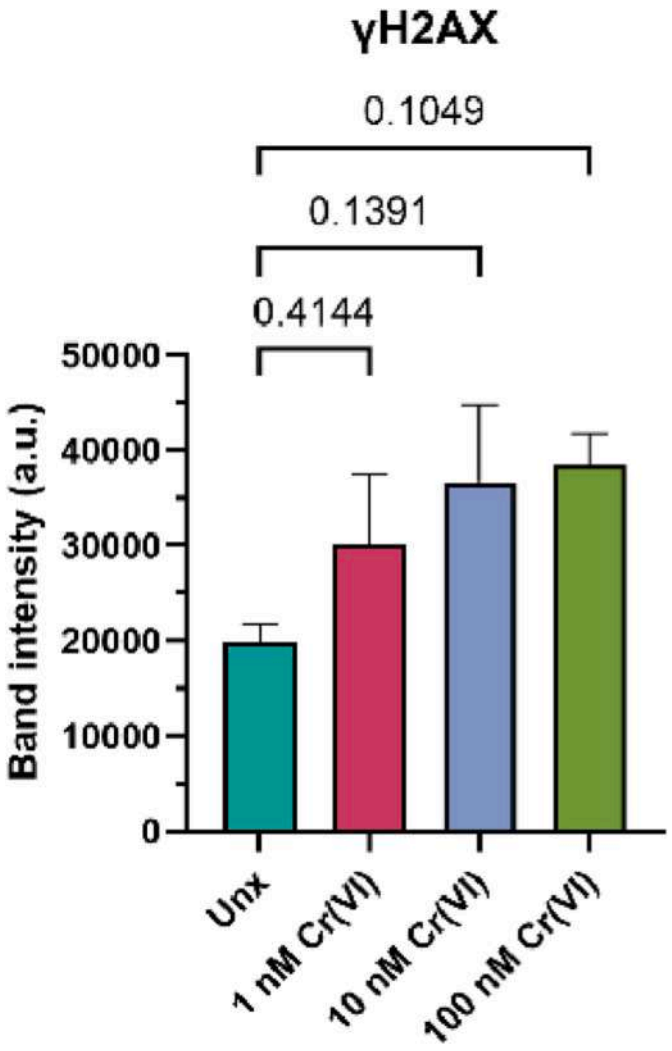

Fig. 4. Western blotting carried out in gonad homogenates of unexposed (Unx) and treated M. galloprovincialis with 1 nM, 10 and 100 nM Cr(VI). Histograms shown a densitometric analyses of γH2A.X bands, reported as mean ± S.D. The differences are not significant. n = 2.

2018 [62]. After 16 h at 4 °C on an orbital shaker, the samples were centrifuged at 14000×*g* for 30 min and then the supernatants containing soluble PL proteins were dialysed with bidistillated water to ensure that all PCA had been removed. The extracted PL proteins were lyophilised and stored at −80 °C.

2.8. Homogenates preparation

Homogenates of the gonads were prepared as described in Bianchi et al. 2023 [63]. The procedures were performed on ice or at 4 °C. The gonad samples (0.3 g) were cut and resuspended in buffer A (1:5 w/v), containing 10 mM Tris-HCl pH 7.5, 1 mM EDTA, 1 mM EGTA, 0.15 mM spermine, 0.75 mM spermidine, 1 mM PMSF, 1 mM β-mercaptoethanol and 2 μg/mL protease inhibitor cocktail. After low-speed homogenization for 20–30 s using an Ultra Turrax T8 (IKA-WERKE), the tissues were centrifuged at 10,000×*g* for 15 min at 4 °C, as described in Vlahogianni et al. 2007 [64]. The supernatant was used for biochemical analysis. The concentration of proteins was determined as reported in Marinaro et al. 2023 [65].

2.9. SDS-PAGE and immunoblotting for γH2A.X analysis

The SDS-PAGE was carried out on polyacrylamide gel 12.9 % (acrylamide/bis-acrylamide 37.5:1, v/v 30 %) in tris-glycine 1X as described in Piscopo et al., 2020 [66] with some changes. Specifically, the stacking gel and the separating gel were 5.0 % and 12.9 % (w/v) acrylamide, respectively, (acrylamide/bis-acrylamide 37.5:1, v/v 30 %). The proteins were then transferred on nitrocellulose filter (0.22 μm) using mini blot system Invitrogen (Waltham, MA, USA). The transfer was performed at 10V for 40 min using a buffer composed by tris-glycine 1X and SDS 0.025 %. This filter was then washed three times for 10 min each time with TBS 1X supplemented with 0.1 % Tween 20. Afterwards, the filter has been incubated for 2 h at room temperature with gelatine 3 % in TBS 1X added with 0.1 % Tween 20. Finally, the filter was washed with TBS 1X containing 0.1 % tween 20. The filter was incubated with primary antibody γH2A.X (Santa Cruz, 938CT5.1.1, sc-517336) in TBS 1X added with 0.1 % Tween 20 and gelatine 0.3 % overnight at 4 °C. Later primary antibody incubation, the filter was washed and incubated with peroxidase (HRP)-conjugated goat anti-mouse IgG (Bioss, BS-0296G-HRP) and the filter was visualized with ECL by ChemiDoc Imaging Systems (Bio-rad). Different times were tested to achieve a correctly exposed filter.

2.10. SDS-PAGE and immunoblotting for PARP and PAR identification

Electrophoresis and Western blotting were performed as follows. All gonad homogenates (20 μg of proteins) were electrophorized at constant current 18 mA on 12 % polyacrylamide slab gel in 0.025 M Tris-0.192 M glycine buffer pH 8.3, containing 0.1 % SDS. 0.1 % Coomassie Brilliant Blue R. was used for gel staining. The proteins separated by SDS-PAGE were then transferred onto a PVDF filter (0.45 μm; Cat No. IPVH00010, Merck Millipore, Milano, Italy) using a Bio-Rad Transblot system (BioRad, Hercules, CA, USA) at constant 200 mA in 0.025 M Tris-0.192 M glycine- 0.025 % SDS buffer, pH 8.6, at 4 °C for 2 h. Monoclonal anti-poly(ADP-ribose)polymerase antibody was used for immunoassay of the blotted PVDF filter (sc-8007, Santa Cruz Biotechnology, Inc., Texas, USA, 1:500) and horseradish peroxidase (HRP)-conjugated anti-mouse secondary antibodies (sc-525409, Santa Cruz Biotechnology, Inc., Texas, USA, 1:2000). HRP reaction was conducted using a kit for chemiluminescence (ECL Western Blotting Substrate, Pierce, 32106, Waltham, MA, USA) and reading by ChemiDoc system (BioRad, Hercules, CA, USA). To remove primary antibodies, PVDF filter was stripped [65]. After repeated washings in Tris-buffered saline (50 mM Tris-HCl and 150 mM NaCl, pH 8.0), the immunoblotting was carried out using monoclonal anti-poly ADP-ribose (PAR) antibody (sc-56198, Santa Cruz, Biotechnology, Inc., Texas, USA, 1:500) and as anti-mouse secondary antibody was utilized horseradish peroxidase (HRP)-conjugated (sc-525409, Santa Cruz Biotechnology, Inc., Texas, USA, 1:2000). PARP and PAR-related signals were quantified through densitometric analysis with Image Lab software (Bio-Rad, Hercules, CA, USA) and reported in terms of optical density (OD; i.e. intensity of one band/mm^2). All experiments were performed at least three times. Electrophoretic analyses showed in Fig. 5 instead, was carried out on 12.8 % polyacrylamide gels.

2.11. PARP activity

PARP activity was measured as reported in Capriello et al. (2022) [4]. The activity assay was set up using a reaction mixture (final volume 50 μL) constituted by 0.5 M Tris-HCl pH 8.0, 50 mM $MgCl_2$, 10 mM DTT, 0.4 mM [^{32}P]NAD^+ (10000 cpm/nmole), and 20 μg protein of all examined samples. The reaction mixture was incubated for 15 min at 25 °C, and subsequently the reaction was stopped on ice after addition of 20 % (w/v) trichloroacetic acid (TCA). The modified and unmodified proteins by PAR were filtered through Millipore filters (HAWPP0001, 0.45 μm) and subjected to repeated washing with 7 % trichloroacetic acid. The determination of acid-insoluble radioactivity (PARP activity) was measured by liquid scintillation in a Beckman counter (model LS 1701) and expressed as mU/g. The enzyme amount required to convert 1 nmol of NAD^+/min under standard conditions represents one enzyme

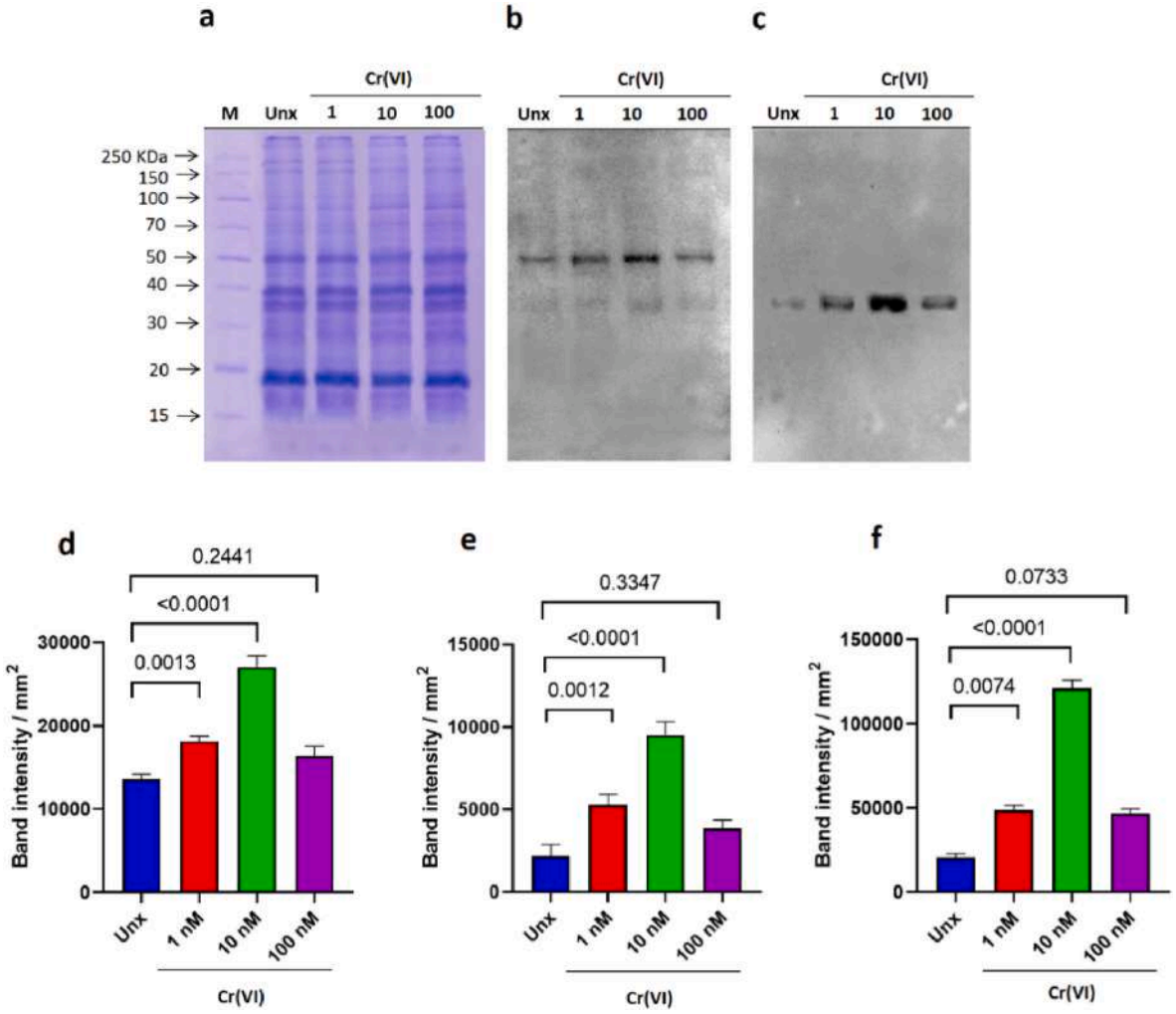

Fig. 5. Western blotting performed in gonad homogenates from unexposed (Unx) and exposed M. galloprovincialis to 1 nM, 10 and 100 nM Cr(VI); (**a**) 12 % (SDS-PAGE); (**b**) anti-PARP immunoblotting; (**c**) anti-PAR immunoblotting; (**d**) densitometric analysis of 50 kDa bands immunopositive to anti-PARP; (**e**) densitometric analysis band immunopositive to anti-PARP with molecular weight between 30 and 40 kDa; (**f**) Kruskal-Wallis test followed by Dunn's multiple comparison test was used to highlight statistically significant differences between gonad homogenates. The data are showed as mean ± SD and the minimum level of acceptable significance was set at $p < 0.05$.

unit. All experiments were repeated for three times.

2.12. Acetic acid urea polyacrylamide gel electrophoresis and western blotting on PL proteins by anti-PAR antibody

The PL proteins were separated by acetic acid urea polyacrylamide gel (AU-PAGE) according to Carbone et al. [67], but with a final concentration of acrylamide of 11.2 % (37.5:1 acrylamide/bis-acrylamide, v/v 30 %). The electrophoresis was carried out at 100V for 1 h. Subsequently, the proteins were transferred from gel to PVDF membrane for 2 h at 4 °C at 100 V. The transfer was performed with 0.7 % acetic acid. Regarding the immunoblotting of H1 histone, the electrophoresis is the same protocol of PL, but the transferred was carried out on nitrocellulose membrane and the blocking was performed with no-fat milk 5 %, as described in Passaro et al. [68]. Finally, anti-PAR polyclonal (Abcam ab14460) and anti-H1 monoclonal antibodies (ABclonal A4342) antibodies was used to conduce the immunoblotting on PVDF membrane and nitrocellulose membrane respectively as described above. The images were acquired by ChemiDoc Imaging Systems (Bio-rad).

2.13. Sperm nuclei preparation and MNase assay

The procedure described by Lettieri et al., 2019 [69] was used to prepare sperm nuclei. Briefly, the sperm pellet was resuspended in 1 mL of a solution consisting of: NaCl 0.15 M; EDTA pH 8 25 mM; PMSF 1 mM. Afterwards the sample was centrifuged for 10 min at 4 °C at 1900×*g* and the supernatant was removed. The pellet obtained was resuspended in 1 mL of solution composed as following: sucrose 0.25 M, $MgCl_2$ 5 mM, TRIS-HCl pH 8 10 mM, PMSF 1 mM, Triton X-100 0.38 %. Subsequently the sample was placed on ice for 10 min and then centrifuged at 1900×*g* at 4 °C for 10 min. The solution containing: 0.25 M sucrose, $MgCl_2$ 5 mM, TRIS-HCl pH 8 10 mM, PMSF 1 mM, was added as final step and after centrifuging at 1900×*g* at 4 °C for 10 min, the sperm nuclei were stored at 4 °C. All concentrations are to be considered final.

2.14. Salt-induced release of M. galloprovincialis SNBP

For the salt-induced release of *M. galloprovincialis* sperm nuclear basic proteins (SNBP) was followed the protocol described in De Guglielmo et al., 2019 [70] The AU-PAGE described in Fioretti et al., 2012 [50] was used to analysed the protein extracts obtained.

2.15. SDS-PAGE for the analysis of M. galloprovincialis PL-proteins

The SDS-PAGE was prepared as following: the stacking gel 4 % (w/v) acrylamide (acrylamide/bis-acrylamide 30:0.2) and the separating gel

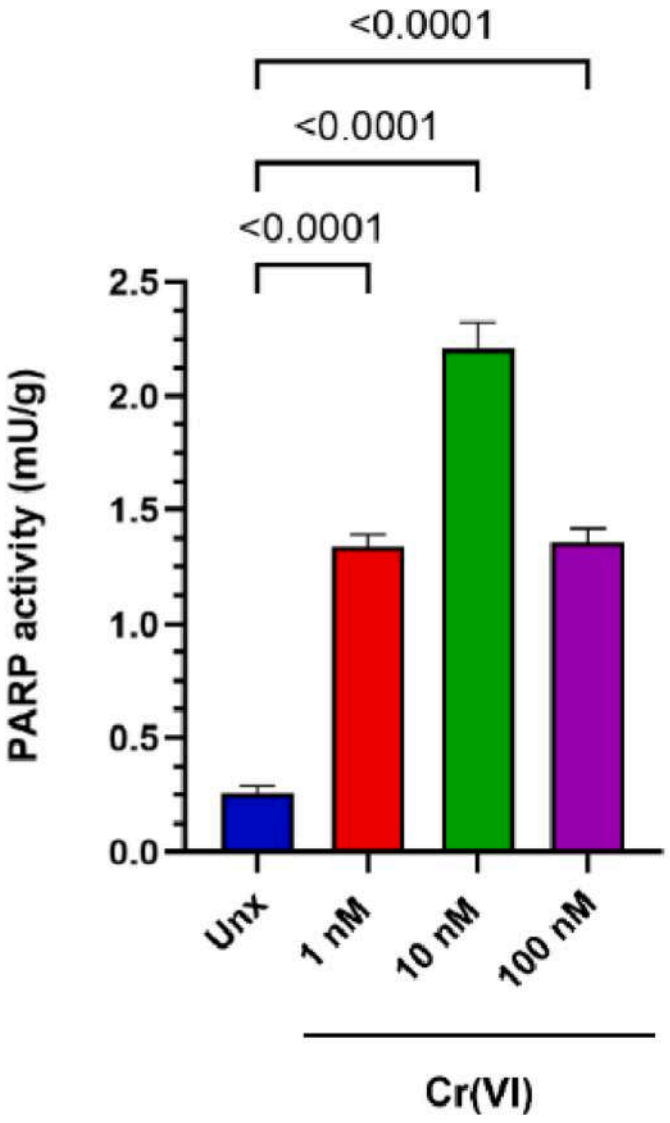

Fig. 6. Poly-ADP-ribose polymerase activity. One-way ANOVA test followed by Tukey's test was used to evaluate statistically significant differences between gonad homogenates. Data expressed as mean ± SD and the minimum level of acceptable significance was set at $p < 0.05$. Unx: unexposed condition.

Table 1
Results of multiple comparison of Dunn's test for 50 kDa band immunopositive to anti-PARP antibody.

Dunn's multiple comparisons test	Significant?	Summary	Adjusted P Value
Unexposed vs. 1 nM Cr (VI)	Yes	**	0,0013
Unexposed vs. 10 nM Cr (VI)	Yes	****	<0,0001
Unexposed vs. 100 nM Cr (VI)	No	ns	0,2441
1 nM Cr (VI) vs. 10 nM Cr (VI)	No	ns	0,2441
1 nM Cr (VI) vs. 100 nM Cr (VI)	No	ns	0,5998
10 nM Cr (VI) vs. 100 nM Cr (VI)	Yes	**	0,0013

11 % (w/v) acrylamide (acrylamide/bis-acrylamide 30:0.2). The running was performed at 100V constant for about 1h. Coomassie Brillant blue was used to stain the gel and the image was acquired by Image Lab (ver. 6.0.1, build 34) software by Gel-doc system. (BioRad, Hercules, CA, USA (BioRad, Hercules, CA, USA).

Table 2
Results of multiple comparison of Dunn's test for 30 kDa band immunopositive to anti-PARP.

Dunn's multiple comparisons test	Significant?	Summary	Adjusted P Value
Unexposed vs. 1 nM Cr (VI)	Yes	**	0,0012
Unexposed vs. 10 nM Cr (VI)	Yes	****	<0,0001
Unexposed vs. 100 nM Cr (VI)	No	ns	0,3347
1 nM Cr (VI) vs. 10 nM Cr (VI)	No	ns	0,2800
1 nM Cr (VI) vs. 100 nM Cr (VI)	No	ns	0,4331
10 nM Cr (VI) vs. 100 nM Cr (VI)	Yes	***	0,0009

2.16. Effect on the DNA absorption spectrum of PL addiction in mussels exposed to Cr(VI)

Absorption spectra of DNA were performed after the addition of PL from 1 nM, 10 nM and 100 nM Cr(VI) exposed mussels following the protocol indicated in Lettieri et al., 2021 [61], by using 1 μg plasmid DNA in 400 μL 1X TBE.

2.17. Statistical analysis

Kruskal-Wallis test was used for PARP expression, then Dunn's multiple comparison test (Fig. 5). ɣH2AX expression and PARP activity instead, was analysed by one-way ANOVA with Tukey's test (Figs. 4 and 6). The values were displays as mean ± SD. Differences $p \leq 0.05$ were considered significant. In the supplementary material are reported the table of multiple comparison for anti-PAR and anti-PARP analyses. The statistical analyses were executed by GraphPad Prism 10.1.0 (316).

3. Results

3.1. Assessment of the accumulation of chromium in the male gonads

Inductively coupled plasma mass spectrometry (ICP-MS) was utilized to evaluate the accumulation of chromium in the male gonads of mussels exposed to Cr(VI). These analyses showed that upon a 24 h exposition to 1, 10 and 100 nM Cr(VI), chromium was found to accumulate in the gonads. Specifically, the quantity of chromium was found to be 0.045 ± 0.0140 μg/g in the gonads of the unexposed animals. The values obtained for the exposed mussels were 0.048 ± 0.0213 μg/g when 1 nM was used, 0.052 ± 0.0116 μg/g when 10 nM was used and 0.072 ± 0.0076 when 100 nM was used (Fig. 1).

3.2. Morphological analyses

Given the accumulation of chromium in the gonad, the possible gonadal damage was determined at morphological level. In unexposed organisms, the testis sections revealed a normal histological architecture, and the cellular composition reflects the reproductive period [71], indeed the spermatic follicles rich in germ cells (GC), in all differentiation stages including spermatozoa (SPZ), are immersed in few connective tissue (Fig. 2a). At the level of cellular interactions, inside the follicles the germ cells were strictly adherent to each other and showed no evidence of disaggregation (Fig. 2a). Testes from animals treated with 1 and 10 nM Cr showed unaltered spermatic follicles even though they began to show signs of tissue distress, in fact infiltrates of hemolymphatic immune cells were evident in the interstitial spaces between the follicles (Fig. 2b–d). The number of immune infiltrates significantly increased in the testes of mussels treated with the highest concentration of Cr, where also structural changes in spermatic follicles have been recorded, showing clear detachment of germ cells from each other and the follicular wall (Fig. 2e). Furthermore, this experimental group showed nodular formations of different immune cells forming a granulomatous structure similar to those observed in vertebrates (Fig. 2f). Finally, PAS staining demonstrated the presence in all treated animals, especially in those exposed to 10 and 100 nM Cr, hyperplastic and

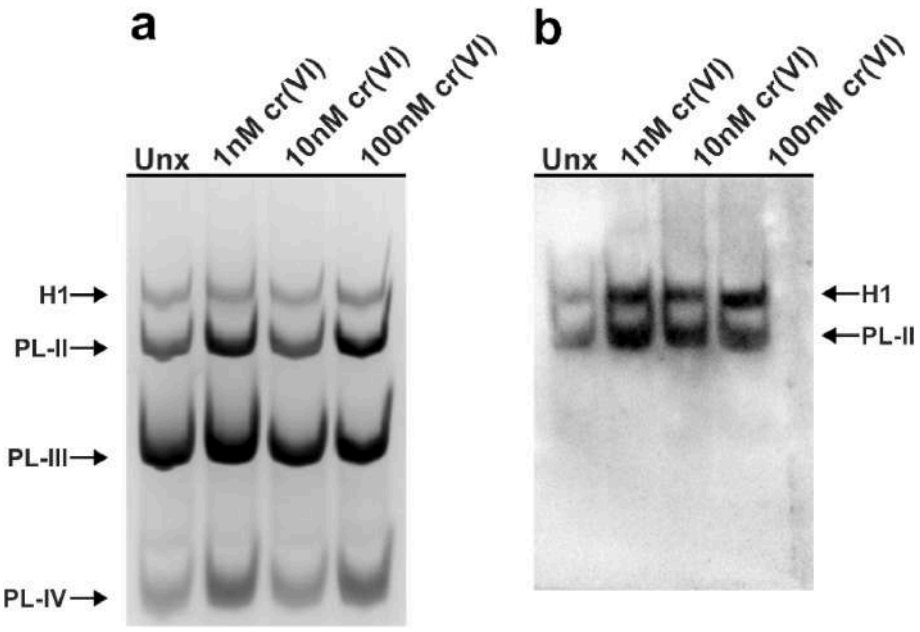

Fig. 7. Western blotting carried out on PL proteins and H1 histone of M. galloprovincialis unexposed (Unx) and exposed to 1 nM, 10 and 100 nMCr(VI). (**a**):11.2 % acetic acid-urea polyacrylamide gel (AU-PAGE). (**b**): anti-PAR immunoblotting.

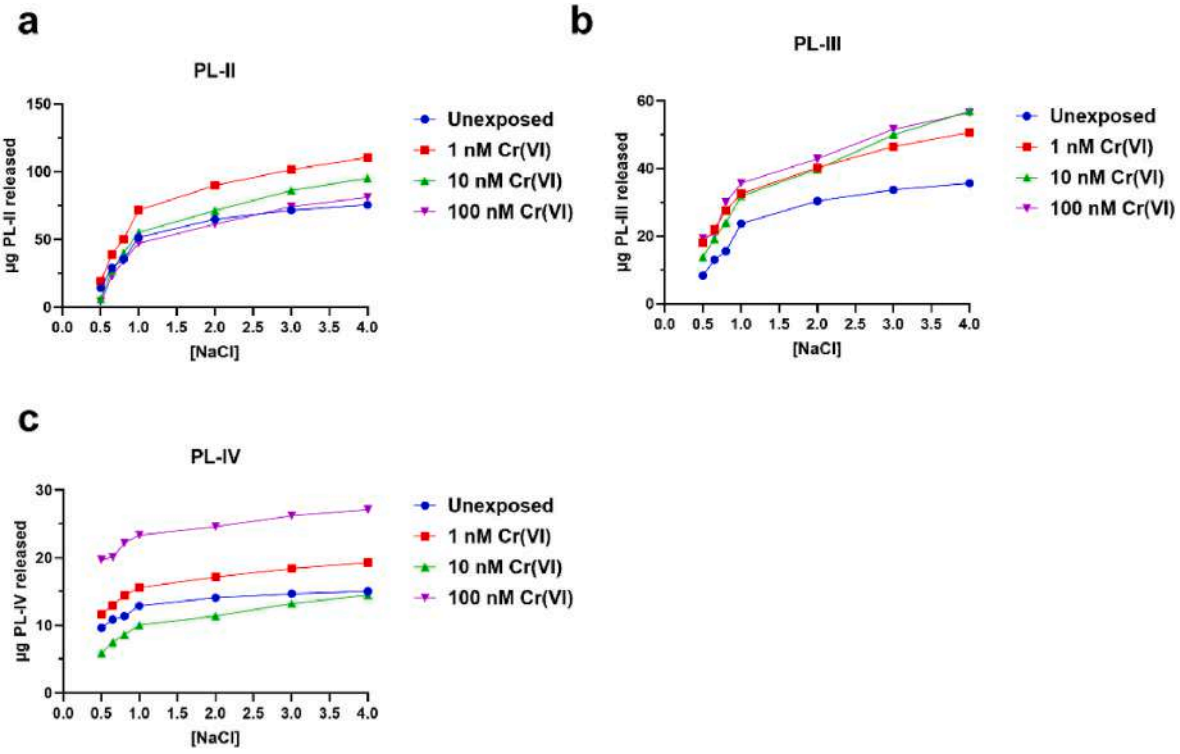

Fig. 8. PL release from sperm nuclei at different molar NaCl concentrations in unexposed (Unx) mussels (blue line, circle) and those exposed to the three concentrations of Cr (VI), 1 nM (red line, square), 10 nM (green line, triangle) and 100 nM (purple line, reversed triangle). (**a**) release of PL-II, (**b**) release of PL-III and (**c**) release of PL-IV.

hypertrophic goblet cells (full of PAS-positive secretion granules) in the connective tissue contour, plus Lipofuscin granules deposited between cells, absent in the unexposed condition and increasing in a dose-related manner in the gonads of Cr-exposed mussels (Fig. 3a–e).

3.3. ɣ*H2A.X expression*

Given the gonadal damage at the morphological level, the level of ɣH2A.X was measured, the latter being a marker of double-stranded damage. Western blotting to evaluate ɣH2A.X expression showed that the increase of the exposure dose resulted in an increase of expression of this protein (Fig. 4).

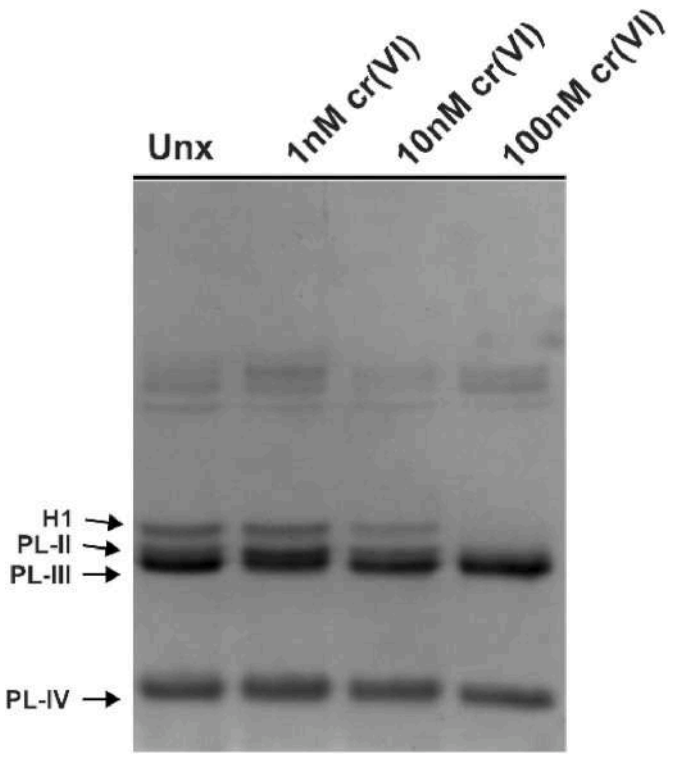

Fig. 9. SDS-PAGE analysis of PL proteins and H1 histone from M. galloprovincialis unexposed (Unx) and exposed to 1 nM, 10 and 100 nM Cr(VI).

3.4. Analysis of PARP expression

PARP expression was evaluated in gonads homogenates of *M. galloprovincialis* exposed to 1, 10 and 100 nM of Cr(VI) doses. Gonad homogenates from unexposed mussels was used as control samples. Electrophoretic analysis of whole tested samples showed that there were no differences in protein quantity and quality (Fig. 5a). Using anti-PARP antibody, two immunopositive bands were identified. One of 50 kDa and the other of 30–40 kDa (Fig. 5b). The densitometric analysis of the immunoreactive bands indicated that the signal intensity of the protein with molecular weight between 30 and 40 kDa (Fig. 5e) in both unexposed and exposed samples to Cr(VI) was weaker than that measured in correspondence of the 50 kDa protein (Fig. 5d). Moreover, in gonadal homogenates of exposed mussels to 1 and 10 nM Cr(VI), the intensity of both immunopositive signals increased significantly compared to the unexposed mussels (Fig. 5d and e). Higher concentrations of Cr(VI) (100 nM) did not cause significant changes in the intensity of either band compared to unexposed mussels. (Fig. 5d and e). Tables 1 and 2, show all multiple comparison of Dunn's test (Supplementary Fig. 1). Immunoblotting by anti-PAR antibody allowed to identify covalent protein acceptors of PAR. In all examined gonad homogenates, the antibody recognized a protein with a molecular weight between 30 and 40 kDa, which is also immunopositive to anti-PARP (Fig. 5c). Although the intensity of this band was greater in all exposed mussels than in unexposed mussels, the highest immunopositive level was found in the sample exposed to 10 nM Cr(VI) (Fig. 5f).

3.5. Enzyme activity of PARP

PARP activity was determined in all examined gonad homogenates to verify whether and how it can be affected by exposure to different doses of Cr(VI). The data showed that exposure at 1 nM and 10 nM Cr (VI) causes a significant increase of enzyme activity compared to unexposed condition. The highest PARP activity was determined at 10 nMCr(VI). In addition, at 100 nM dose, PARP activity was significantly lower than that measured in the mussels exposed to 10 nMCr(VI), however it remained significantly higher compared to unexposed mussels and comparable to that obtained at 1 nM (Fig. 6).

3.6. Poly(ADPribosyl)ation of PL proteins

PL proteins extract from all examined *M. galloprovincialis* gonads were separated by AU-PAGE (Fig. 7a) and subjected to immunoblotting

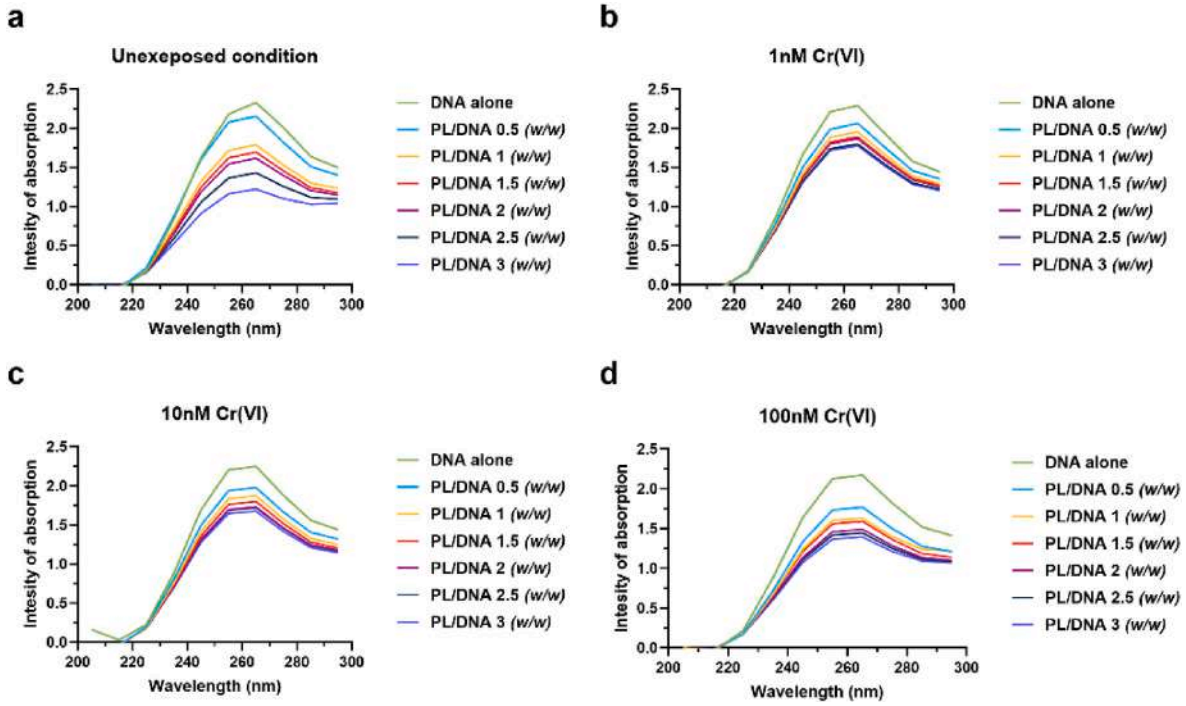

Fig. 10. Absorption spectra of plasmid DNA alone and PL/DNA mixtures at different PL/DNA ratios in the 200–300 nm range: PL extracts from unexsposed mussels (a) and PL extracts of mussels with exposure to 1 nM (b), 10 nM (c) and 100 nM Cr(VI) (d).

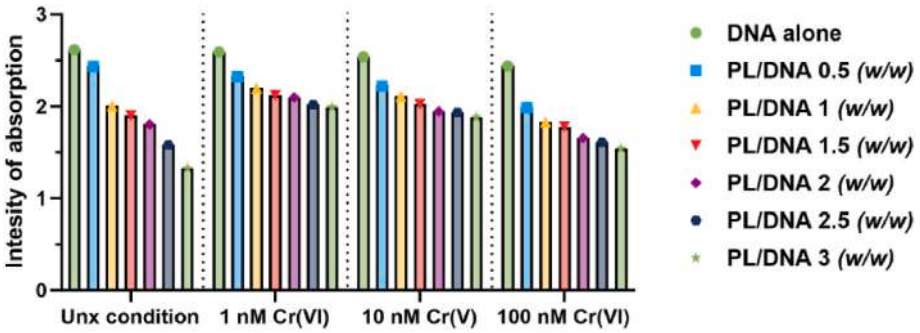

Fig. 11. Histogram of absorption DNA peak for each PL/DNA (w/w) ratios.

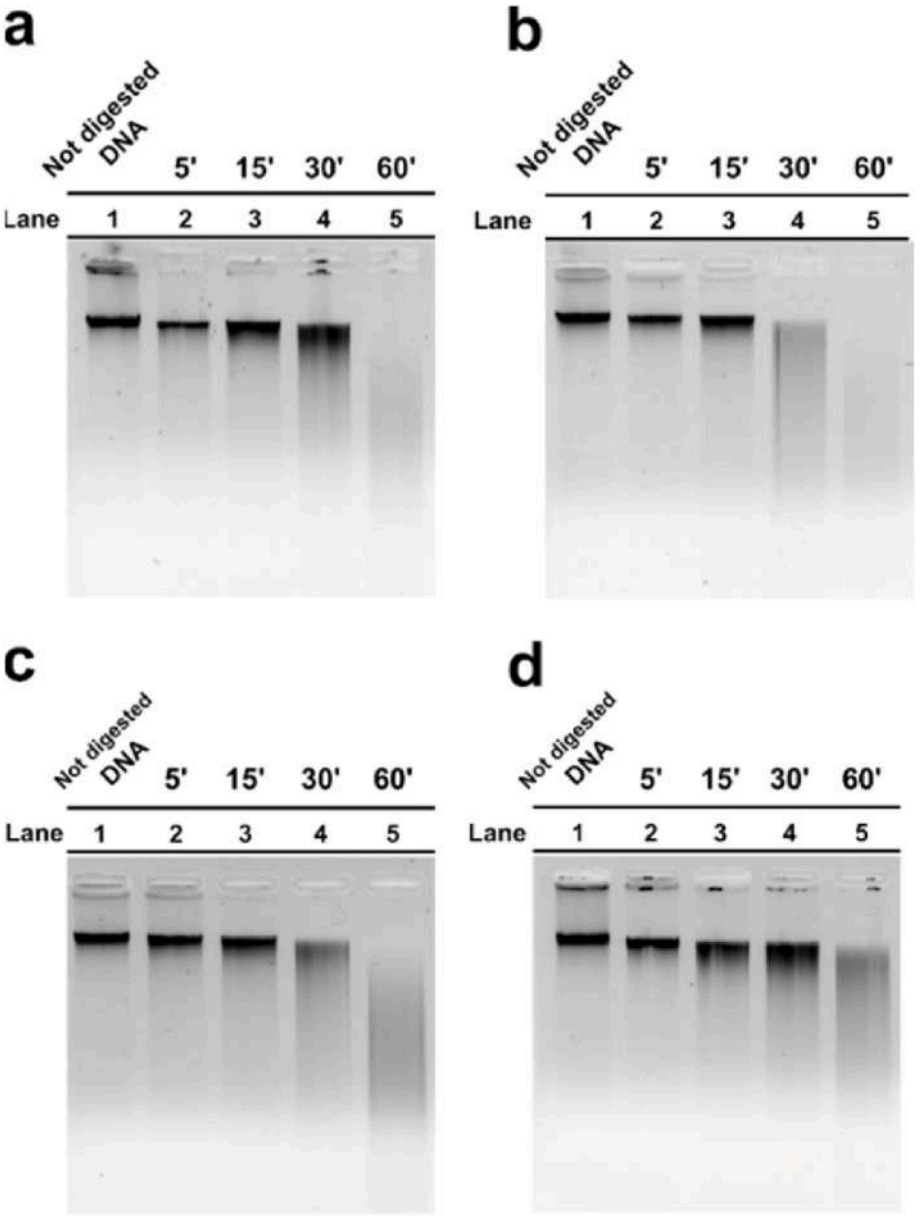

Fig. 12. Agarose gel (0.9 %) analysis of chromatin digestion time-course products with MNase of sperm nuclei from unexposed and exposed mussels. (**a**) unexposed condition; (**b**)1 nM Cr(VI), (**c**) 10 nM Cr(VI), (**d**) 100 nM Cr(VI) condition.

with anti-PAR antibody (Fig. 7b), to investigate whether PL proteins were endogenously modified with ADPR polymers. Two immunopositive signals were observed in all samples, PL-II and H1 histone. The electrophoretic band with lower mobility respect to PL-II corresponding H1 histone was demonstrated by immunoblotting with anti-H1 antibody (Supplementary Fig. S1)

3.7. Release of PL from sperm nuclei by salt solution

Given the Poly(ADPribosyl)ation of PL-II observed after chromium exposure, the changes in PL-DNA binding were investigated. For this purpose, we tested how PLs were released from sperm nuclei (Fig. 8) in mussels exposed and unexposed by using increasing concentrations of NaCl. This analysis indicated that PL-II (Fig. 8a), after having exposed mussels to 100 nM Cr(VI) was released in very similar amounts with respect to unexposed condition, and in greater amounts after exposure to 10 and 1 nM Cr(VI), where at 1 nM a greater release was observed compared to 10 nM. In contrast, PL-III (Fig. 8b) shows greater release after exposing mussels to all doses matched to unexposed condition. PL-IV (Fig. 8c), on the other hand, was released in larger amounts after exposure to 1 and 100 nM Cr (VI) respect to the unexposed condition, where at 100 nM a greater release respect to all the other conditions was observed.

3.8. Electrophoretic analyses of PL by SDS-PAGE

The analysis of PL proteins by SDS-PAGE exhibited a complete co-migration of H1, PL-II and PL-III in mussels that were exposed to 100 nM; in contrast, in the 1 and 10 nM Cr(VI) exposure conditions, the electrophoretic pattern was similar to the unexposed (Unx) condition (Fig. 9).

3.9. Absorption spectrum of DNA after the addition of PL proteins

To evaluate possible effects of exposure of mussels to Cr(VI) on the ability of PL proteins to bind to DNA, the absorption spectrum in the 200–300 nm range of plasmid DNA lonely was equated with the absorption spectra of the same after addition of increasing amounts of PL (0.5-1-1.5-2-3 PL/DNA (w/w) ratios) from unexposed (Fig. 10a) and Cr (VI)-exposed (Fig. 10b–d) mussels. PL proteins derived from exposed mussels showed reduced DNA binding compared to PL proteins from unexposed mussels, as shown in Fig. 10b–d. This could indicate changes in the binding of PL-DNA after exposure to Cr(VI). The absorption peaks for each PL/DNA ratio (w/w) are shown in Fig. 11, where the different decrease in DNA absorption between unexposed and exposed conditions is clearly visible.

3.10. Sperm chromatin digestion by micrococcal nuclease

Possible Cr(VI)-induced alterations in sperm chromatin were investigated using micrococcal nuclease (MNase) and performing a time-course of digestion. As shown in Fig. 12, in unexposed mussels, DNA was progressively degraded as digestion times increase under our experimental conditions (Fig. 12a). Following exposure to doses of 1 nM (Figs. 12b) and 10 nM Cr (VI) (Fig. 12c), the sperm chromatin DNA appeared to show increased accessibility to micrococcal nuclease while a very similar result respect to unexposed condition was observed after exposure to 100 nM Cr(VI) (Fig. 12d).

4. Discussion

Epigenetic modifications are pivotal to the metabolism of DNA, and in the last few years PARP and PARylation have gained an increasingly central role in the remodelling of chromatin. PARylation is commonly associated with DNA repair, but the role of PARylation in sperm chromatin remains to be elucidated. In the present work we demonstrated that *M. galloprovincialis* exposure to 1, 10 and 100 nM Cr(VI) doses influenced PARP expression and enzyme activity. In detail, the gonad homogenates of unexposed and exposed mussels indicated the presence of two PARPs isoforms, one with a molecular weight of 50 kDa and the other with a molecular weight ranged 30–40 kDa, both already identified in *M. galloprovincialis* [72]. The increase of PARP expression and activity measured in the gonads of the mussels exposed to 1 nM and 10 nM of Cr(VI) allows us to hypothesize that already low doses of this metal were capable of inducing oxidative damage to genomic material. It seems also plausible to assume that the PARP activity and its automodification increase are correlated to genomic material damage entity [73]. On the other hand, the PARP activation under stress conditions and its correlation with pollution was already widely demonstrated in both animals and plants [4,7,74–77]. Interestingly, the most oxidative DNA damage would occur at 10 nM chromium dose, at which the highest activity and maximum automodification of the enzyme was detected. At higher doses of chromium (100 nM), mussels could adopt the strategy of reducing the activity of PARP, recognized as being one of the most important cellular energy consumers, in order to maintain energy homeostasis, necessary for their survival. In addition, for the first time, we demonstrated endogenous heteromodification by poly(ADPribosyl)ation of PL proteins obtained from exposed and unexposed samples. In detail, the anti-PAR immunopositive signal corresponding to a protein with higher electrophoretic migration we know corresponds to PL-II, while the signal with lower migration corresponds to H1 histone. This modification is very common in the H1 histone, but it is new for PL-II. This latter protein plays an important part in organising the chromatin of *M. galloprovincialis* spermatozoa by interacting with linker DNA [78] and is required for the high degree of compaction reached by the Mytilus sperm nucleus, as revealed by electron micrographs of the spread nuclei [79]. The evidence that the intensity of the signal was always higher in the exposed samples than the control leads us to hypothesize that, following the DNA damage caused by the exposure to chromium, the PL-II is heteromodified, as well as the histone H1, with poly(ADPR) and its poly(ADPribosyl)ation is related to the decondensation of chromatin and its repair [12,17–19]. Therefore, DNA damage induced by exposure to chromium (VI) leads to activation of poly (ADPribosyl)ation, with consequent automodification of PARP and heteromodification of PL-II by poly(ADPR) polymers. These data allow us to assume that PAR bound to PARP acts as a signaller of damage to genomic material and attracts the enzymes involved in repair, after chromatin relaxation following PLII heteromodification. Starting from this evidence, gonadal H2A.X phosphorylation (ɣH2A.X), another marker of DNA damage, was also evaluated. In fact, an immediate phosphorylation by the Map kinase enzyme cascade of this histone occurs, favouring the recruitment of the enzymes and protein complexes responsible for DNA damage resolution [80]. Our data highlighted an increase in the expression of ɣH2A.X dose-dependent on chromium exposure. Since both poly(ADPribosyl)ation and phosphorylation are two modifications activated by genotoxic damage, we wanted to verify whether and what relationship might exist between them. In this regard, we propose a molecular model in which hypothesize, that at low chromium concentrations both modifications are activated following genotoxic damage and act as signals for the recruitment of factors involved in DNA repair. This hypothesis seems to be also confirmed by MNase data, which showed a major accessibility of MNase to sperm DNA. At high chromium concentrations, instead, the concomitant decrease in PARP activity and increase in ɣH2A.X could indicate the possibility that, although poly(ADPribosyl)ation continues to ensure chromatin relaxation, the phosphorylation becomes the main player in its repair. After exposure to 100 nM Cr(VI), however, the phosphorylation does not seem to be able to repair all the damaged DNA, thus damage proceeds at level of the gonads, as clearly shown by morphological data. In detail, histological investigations recorded gonadal damage with a dose-dependent trend. The most significant alterations found are represented by a structural disorganisation of the germ cells within spermatic follicles and the presence of haemocyte infiltrates in the gonadic connective tissue. The disconnection between the cells within the spermatic follicles agrees with the literature, in fact, it is a well-known fact that heavy metals are detrimental to the process of spermatogenesis; between the numerous types of damage that have been observed, the disruption of the blood-testicular barrier and of cell junctions has been described [65,81]. The presence of many haemocytes in the

testicular connective tissue, particularly in the testis of mussels exposed to 100 nM Cr, where the evidence for the presence of haemocytes clustered in the formation of a granulomatous structures is also detected, suggests strong inflammation of the gonad caused by the metal accumulation [82]. The inflammatory process and the stress condition are also confirmed by the presence of PAS-positive cells with a dose-dependent trend in the exposed animals. It is known that, in molluscs, under stress conditions a large release of mucus is observed through goblet cells, cells positive to PAS staining, which appear hypertrophic and more numerous [83]. It is very likely that the inflammatory process just described could be triggered by Cr-induced oxidative stress phenomena. Indeed, PAS staining also revealed the presence of lipofuscin granules in animals exposed to Cr especially at concentration of 100 nM. These granules are high-molecular weight formations of protein aggregates. There is much evidence that the formation of lipofuscin aggregates is a direct condition of oxidative stress. Indeed, under normal conditions, most protein aggregates are ubiquitinated by the proteasome and subsequently eliminated [84]. On the contrary, highly oxidised and cross-linked proteins are unfavourable substrates for the proteasome, which in turn is inhibited by this type of formation; therefore, these aggregates are not ubiquitinated, forming evident cellular precipitates of coloured granules known as lipofuscin granules [84]. Considering all data obtained on gonadal tissue, we hypothesized that chromium could affect PL proteins-DNA binding, which is critical in the compaction of sperm chromatin. As a matter of fact, compared to unexposed mussels, the released PL from sperm nuclei at increasing NaCl molarities indicates changes in PL binding to sperm DNA, as an increase in the amount of PL released from sperm nuclei was almost always observed under exposed conditions. For this experimental approach, the only condition most similar to the unexposed condition was for PL-II at a Cr(VI) exposure dose of 100 nM. This last result could be due to the observation of a complete SDS-PAGE co-migration of PL-II with PL-III and H1 histone only in this condition. The explanation could be due to the conformational changes of the PL proteins induced by chromium, as already reported by Marinaro et al., 2023 [85]. Considering these conformational changes in PLs, we performed turbidimetric measurements under all conditions tested to obtain further evidence of alterations in PL-DNA binding induced by exposure of mussels to chromium. The results obtained showed a reduction in the ability of PL to bind the DNA of mussels that were exposed to the three doses of Cr(VI). In fact, a lowering of the absorbance peak at 260 nm was observed, and more clearly at the 1 and 10 nM Cr(VI) exposure conditions. The structure of the chromatin of spermatozoa may be affected by changes in the binding of PL to DNA which in turn influence the locomotion of male gametes and consequently also their ability to fertilise oocytes. In fact, an increase in the accessibility of sperm chromatin to this enzyme after 1 and 10 nM Cr (VI) exposure was observed. These results suggest that the exposure of mussels to these doses of Cr(VI) leads to a series of molecular alterations in PL, which affect their binding to DNA and influence the sperm chromatin. In addition, these Cr(VI) exposure doses induce gonadal damage as indicated by the PARP and γH2A.X markers alterations. Although many investigations are still needed to define the precise mechanisms of action leading to the damage produced by chromium, the results of this work add new insights into the possible molecular mechanism underlying the effects of chromium on *M. galloprovincialis*. reproductive system.

CRediT authorship contribution statement

Carmela Marinaro: Writing – review & editing, Writing – original draft, Visualization, Software, Investigation, Formal analysis, Data curation. **Alberto Marino:** Writing – original draft, Investigation. **Anna Rita Bianchi:** Writing – review & editing, Writing – original draft, Investigation, Data curation. **Bruno Berman:** Investigation, Data curation. **Marco Trifuoggi:** Visualization, Supervision, Resources. **Alessandra Marano:** Writing – original draft, Investigation. **Giancarlo Palumbo:** Writing – review & editing, Writing – original draft. **Teresa Chianese:** Writing – original draft, Visualization, Investigation, Formal analysis. **Rosaria Scudiero:** Validation, Supervision, Resources, Methodology. **Luigi Rosati:** Writing – review & editing, Writing – original draft, Validation, Supervision, Resources, Methodology, Conceptualization. **Anna De Maio:** Writing – review & editing, Writing – original draft, Validation, Supervision, Resources, Project administration, Methodology, Conceptualization. **Gennaro Lettieri:** Writing – review & editing, Writing – original draft, Visualization, Software, Methodology, Investigation, Formal analysis, Data curation. **Marina Piscopo:** Writing – review & editing, Writing – original draft, Validation, Supervision, Resources, Project administration, Methodology, Conceptualization.

Declaration of competing interest

The authors declare that they have no known competing financial interests or personal relationships that could have appeared to influence the work reported in this paper.

Data availability

Data will be made available on request.

Appendix A. Supplementary data

Supplementary data to this article can be found online at https://doi.org/10.1016/j.cbi.2024.111186.

References

[1] T. Eisemann, J.M. Pascal, Poly(ADP-ribose) polymerase enzymes and the maintenance of genome integrity, Cell. Mol. Life Sci. 77 (2020) 19–33, https://doi.org/10.1007/s00018-019-03366-0.
[2] C. Arena, V. De Micco, A. De Maio, Growth alteration and leaf biochemical responses in *Phaseolus vulgaris* exposed to different doses of ionising radiation, Plant Biol. 16 (Suppl 1) (2014) 194–202, https://doi.org/10.1111/plb.12076.
[3] C. Arena, A. de maio, F. De Nicola, L. Santorufo, L. Vitale, G. Maisto, Assessment of eco-physiological performance of *Quercus ilex L. Leaves* in urban area by an integrated approach, Water, Air, Soil Pollut. 225 (2013), https://doi.org/10.1007/s11270-013-1824-6.
[4] T. Capriello, G. Di Meglio, A. De Maio, R. Scudiero, A.R. Bianchi, M. Trifuoggi, M. Toscanesi, A. Giarra, I. Ferrandino, Aluminium exposure leads to neurodegeneration and alters the expression of marker genes involved to parkinsonism in zebrafish brain, Chemosphere 307 (2022) 135752, https://doi.org/10.1016/j.chemosphere.2022.135752.
[5] G. D'Errico, G. Vitiello, G. De Tommaso, F.K. Abdel-Gawad, M.V. Brundo, M. Ferrante, A. De Maio, S. Trocchia, A.R. Bianchi, G. Ciarcia, G. Guerriero, Electron Spin Resonance (ESR) for the study of Reactive Oxygen Species (ROS) on the isolated frog skin (*Pelophylax bergeri*): a non-invasive method for environmental monitoring, Environ. Res. 165 (2018) 11–18, https://doi.org/10.1016/j.envres.2018.03.044.
[6] G. Guerriero, G. D'Errico, A.D. Maio, A. RitaBianchi, O.S. Olanrewaju, G. Ciarcia, G. Guerriero, G. D'Errico, A.D. Maio, A. RitaBianchi, O.S. Olanrewaju, G. Ciarcia, Soil Remediation Assessment by Detection of Reactive Oxygen Species in Lizard Testis: an Electron Spin Resonance (ESR) Approach, IntechOpen, 2018, https://doi.org/10.5772/intechopen.72337.
[7] A. De Maio, S. Trocchia, G. Guerriero, The amphibian Pelophylax bergeri (Günther, 1986) testis poly(ADP-ribose)polymerases: relationship to endocrine disruptors during spermatogenesis, Ital. J. Zool. 81 (2014) 256–263, https://doi.org/10.1080/11250003.2014.902124.
[8] O.S. Olanrewaju, A. De Maio, E. Lionetti, A.R. Bianchi, D. Rabbito, A. Ariano, F.-Z. Majdoubi, G. Guerriero, Sea farms as a safe and sustainable food source: an investigation on use of Seaweeds for liver detoxification and reduced DNA damage in Lates calcarifer (bloch, 1790), in: M. Ksibi, A. Ghorbal, S. Chakraborty, H. I. Chaminé, M. Barbieri, G. Guerriero, O. Hentati, A. Negm, A. Lehmann, J. Römbke, A. Costa Duarte, E. Xoplaki, N. Khélifi, G. Colinet, J. Miguel Dias, I. Gargouri, E.D. Van Hullebusch, B. Sánchez Cabrero, S. Ferlisi, C. Tizaoui, A. Kallel, S. Rtimi, S. Panda, P. Michaud, J.N. Sahu, M. Seffen, V. Naddeo (Eds.), Recent Advances in Environmental Science from the Euro-Mediterranean and Surrounding Regions, second ed., Springer International Publishing, Cham, 2021, pp. 671–675, https://doi.org/10.1007/978-3-030-51210-1_106.
[9] E.E. Alemasova, O.I. Lavrik, Poly(ADP-ribosyl)ation by PARP1: reaction mechanism and regulatory proteins, Nucleic Acids Res. 47 (2019) 3811–3827, https://doi.org/10.1093/nar/gkz120.
[10] M. Tallis, R. Morra, E. Barkauskaite, I. Ahel, Poly(ADP-ribosyl)ation in regulation of chromatin structure and the DNA damage response, Chromosoma 123 (2014) 79–90, https://doi.org/10.1007/s00412-013-0442-9.

[11] O.S. Olanrewaju, O. Oyatomi, O.O. Babalola, M. Abberton, GGE biplot analysis of genotype × environment interaction and yield stability in Bambara groundnut, Agronomy 11 (2021) 1839, https://doi.org/10.3390/agronomy11091839.
[12] N. Ogata, K. Ueda, M. Kawaichi, O. Hayaishi, Poly(ADP-ribose) synthetase, a main acceptor of poly(ADP-ribose) in isolated nuclei, J. Biol. Chem. 256 (1981) 4135–4137.
[13] G.G. Poirier, G. de Murcia, J. Jongstra-Bilen, C. Niedergang, P. Mandel, Poly(ADP-ribosyl)ation of polynucleosomes causes relaxation of chromatin structure, Proc. Natl. Acad. Sci. U. S. A. 79 (1982) 3423–3427, https://doi.org/10.1073/pnas.79.11.3423.
[14] G. Krupitza, P. Cerutti, Poly(ADP-ribosylation) of histones in intact human keratinocytes, Biochemistry 28 (1989) 4054–4060, https://doi.org/10.1021/bi00435a063.
[15] P. Adamietz, A. Rudolph, ADP-ribosylation of nuclear proteins in vivo. Identification of histone H2B as a major acceptor for mono- and poly(ADP-ribose) in dimethyl sulfate-treated hepatoma AH 7974 cells, J. Biol. Chem. 259 (1984) 6841–6846, https://doi.org/10.1016/S0021-9258(17)39804-6.
[16] M.L. Nosella, T.H. Kim, S.K. Huang, R.W. Harkness, M. Goncalves, A. Pan, M. Tereshchenko, S. Vahidi, J.L. Rubinstein, H.O. Lee, J.D. Forman-Kay, L.E. Kay, Poly(ADP-ribosyl)ation enhances nucleosome dynamics and organizes DNA damage repair components within biomolecular condensates, Mol. Cell 84 (2024) 429–446.e17, https://doi.org/10.1016/j.molcel.2023.12.019.
[17] R.J. Aubin, V.T. Dam, J. Miclette, Y. Brousseau, A. Huletsky, G.G. Poirier, Hyper (ADP-ribosyl)ation of histone H1, Can. J. Biochem. 60 (1982) 1085–1094, https://doi.org/10.1139/o82-139.
[18] T. Ushiroyama, Y. Tanigawa, M. Tsuchiya, R. Matsuura, M. Ueki, O. Sugimoto, M. Shimoyama, Amino acid sequence of histone H1 at the ADP-ribose-accepting site and ADP-ribose ·histone-H1 adduct as an inhibitor of cyclic-AMP-dependent phosphorylation, Eur. J. Biochem. 151 (1985) 173–177, https://doi.org/10.1111/j.1432-1033.1985.tb09082.x.
[19] S. Messner, M. Altmeyer, H. Zhao, A. Pozivil, B. Roschitzki, P. Gehrig, D. Rutishauser, D. Huang, A. Caflisch, M.O. Hottiger, PARP1 ADP-ribosylates lysine residues of the core histone tails, Nucleic Acids Res. 38 (2010) 6350–6362, https://doi.org/10.1093/nar/gkq463.
[20] M. Malanga, L. Atorino, F. Tramontano, B. Farina, P. Quesada, Poly(ADP-ribose) binding properties of histone H1 variants, Biochim. Biophys. Acta Gene Struct. Expr. 1399 (1998) 154–160, https://doi.org/10.1016/S0167-4781(98)00110-9.
[21] N. Ogata, K. Ueda, O. Hayaishi, ADP-ribosylation of histone H2B. Identification of glutamic acid residue 2 as the modification site, J. Biol. Chem. 255 (1980) 7610–7615.
[22] A. Kreimeyer, K. Wielckens, P. Adamietz, H. Hilz, DNA repair-associated ADP-ribosylation in vivo. Modification of histone H1 differs from that of the principal acceptor proteins, J. Biol. Chem. 259 (1984) 890–896.
[23] G. Lettieri, C. Marinaro, C. Brogna, L. Montano, M. Lombardi, A. Trotta, J. Troisi, M. Piscopo, A metabolomic analysis to assess the responses of the male gonads of *Mytilus galloprovincialis* after heavy metal exposure, Metabolites 13 (2023) 1168, https://doi.org/10.3390/metabo13121168.
[24] G. Lettieri, C. Marinaro, R. Notariale, P. Perrone, M. Lombardi, A. Trotta, J. Troisi, M. Piscopo, Impact of heavy metal exposure on *Mytilus galloprovincialis* spermatozoa: a metabolomic investigation, Metabolites 13 (2023) 943, https://doi.org/10.3390/metabo13080943.
[25] M. Piscopo, R. Notariale, D. Rabbito, J. Ausió, O.S. Olanrewaju, G. Guerriero, Mytilus galloprovincialis (Lamarck, 1819) spermatozoa: hsp70 expression and protamine-like protein property studies, Environ. Sci. Pollut. Res. 25 (2018) 12957–12966, https://doi.org/10.1007/s11356-018-1570-9.
[26] C. Jeandel, J.-F. Minster, Isotope dilution measurement of inorganic chromium(III) and total chromium in seawater, Mar. Chem. 14 (1984) 347–364, https://doi.org/10.1016/0304-4203(84)90030-6.
[27] D.R. Livingstone, Contaminant-stimulated reactive oxygen species production and oxidative damage in aquatic organisms, Mar. Pollut. Bull. 42 (2001) 656–666, https://doi.org/10.1016/s0025-326x(01)00060-1.
[28] A. Chiu, X.L. Shi, W.K.P. Lee, R. Hill, T.P. Wakeman, A. Katz, B. Xu, N.S. Dalal, J. D. Robertson, C. Chen, N. Chiu, L. Donehower, Review of chromium (VI) apoptosis, cell-cycle-arrest, and carcinogenesis, J. Environ. Sci. Health C Environ. Carcinog. Ecotoxicol. Rev. 28 (2010) 188–230, https://doi.org/10.1080/10590501.2010.504980.
[29] G. Wang, C. Zhang, B. Huang, Transcriptome analysis and histopathological observations of *Geloina erosa* gills upon Cr(VI) exposure, Comp. Biochem. Physiol. C Toxicol. Pharmacol. 231 (2020) 108706, https://doi.org/10.1016/j.cbpc.2020.108706.
[30] V. Singh, N. Singh, M. Verma, R. Kamal, R. Tiwari, M. Sanjay Chivate, S.N. Rai, A. Kumar, A. Singh, M.P. Singh, E. Vamanu, V. Mishra, Hexavalent-chromium-induced oxidative stress and the protective role of antioxidants against cellular toxicity, Antioxidants 11 (2022) 2375, https://doi.org/10.3390/antiox11122375.
[31] P. Perrone, G. Lettieri, C. Marinaro, V. Longo, S. Capone, A. Forleo, S. Pappalardo, L. Montano, M. Piscopo, Molecular alterations and severe abnormalities in spermatozoa of young men living in the "valley of sacco river" (latium, Italy): a preliminary study, Int. J. Environ. Res. Publ. Health 19 (2022) 11023, https://doi.org/10.3390/ijerph191711023.
[32] K.E. Ukhurebor, U.O. Aigbe, R.B. Onyancha, W. Nwankwo, O.A. Osibote, H. K. Paumo, O.M. Ama, C.O. Adetunji, I.U. Siloko, Effect of hexavalent chromium on the environment and removal techniques: a review, J. Environ. Manag. 280 (2021) 111809, https://doi.org/10.1016/j.jenvman.2020.111809.
[33] I.-P.D. Eliopoulos, G.D. Eliopoulos, M. Economou-Eliopoulos, The Cr(VI) stability in contaminated coastal groundwater: salinity as a driving force, Minerals 11 (2021) 160, https://doi.org/10.3390/min11020160.
[34] H. Elderfield, Chromium speciation in sea water, Earth Planet Sci. Lett. 9 (1970) 10–16, https://doi.org/10.1016/0012-821X(70)90017-8.
[35] D. Grimaud, G. Michard, Concentration du chrome dans deux profils de l'ocean pacifique, Mar. Chem. 2 (1974) 229–237, https://doi.org/10.1016/0304-4203(74)90017-6.
[36] R.E. Cranston, J.W. Murray, Chromium species in the columbia river and estuary1, Limnol. Oceanogr. 25 (1980) 1104–1112, https://doi.org/10.4319/lo.1980.25.6.1104.
[37] M. Piscopo, Seasonal dependence of cadmium molecular effects on *Mytilus galloprovincialis* (Lamarck, 1819) protamine-like protein properties, Mol. Reprod. Dev. 86 (2019) 1418–1429, https://doi.org/10.1002/mrd.23240.
[38] C.-H. Lee, T.-K. Ryu, M. Chang, J.-W. Choi, Effect of silver, cadmium, chromium, copper, and zinc on the fertilization of the northern pacific asteroid, *Asterias amurensis*, Bull. Environ. Contam. Toxicol. 73 (2004), https://doi.org/10.1007/s00128-004-0472-3.
[39] L. Li, H. Chen, R. Bi, L. Xie, Bioaccumulation, subcellular distribution, and acute effects of chromium in Japanese medaka (*Oryzias latipes*), Environ. Toxicol. Chem. 34 (2015) 2611–2617, https://doi.org/10.1002/etc.3112.
[40] H. Chen, J. Cao, L. Li, X. Wu, R. Bi, P.L. Klerks, L. Xie, Maternal transfer and reproductive effects of Cr(VI) in Japanese medaka (*Oryzias latipes*) under acute and chronic exposures, Aquat. Toxicol. 171 (2016) 59–68, https://doi.org/10.1016/j.aquatox.2015.12.011.
[41] P.M. Basha, V. Latha, Evaluation of sublethal toxicity of zinc and chromium in *Eudrilus eugeniae* using biochemical and reproductive parameters, Ecotoxicology 25 (2016) 802–813, https://doi.org/10.1007/s10646-016-1637-7.
[42] G. Lettieri, R. Notariale, A. Ambrosino, A. Di Bonito, A. Giarra, M. Trifuoggi, C. Manna, M. Piscopo, Spermatozoa transcriptional response and alterations in PL proteins properties after exposure of *Mytilus galloprovincialis* to mercury, Int. J. Mol. Sci. 22 (2021) 1618, https://doi.org/10.3390/ijms22041618.
[43] C. Moriello, M. Costabile, M. Spinelli, A. Amoresano, G. Palumbo, F. Febbraio, M. Piscopo, Altered expression of protamine-like and their DNA binding induced by Cr(VI): a possible risk to spermatogenesis? Biomolecules 12 (2022) 700, https://doi.org/10.3390/biom12050700.
[44] G. Lettieri, N. Carusone, R. Notariale, M. Prisco, A. Ambrosino, S. Perrella, C. Manna, M. Piscopo, Morphological, gene, and hormonal changes in gonads and in-creased micrococcal nuclease accessibility of sperm chromatin induced by mercury, Biomolecules 12 (2022) 87, https://doi.org/10.3390/biom12010087.
[45] A.D. Nunzio, A. Giarra, M. Toscanesi, A. Amoresano, M. Piscopo, E. Ceretti, C. Zani, S. Lorenzetti, M. Trifuoggi, L. Montano, Comparison between macro and trace element concentrations in human semen and blood serum in highly polluted areas in Italy, Int. J. Environ. Res. Publ. Health 19 (2022) 11635, https://doi.org/10.3390/ijerph191811635.
[46] G. Ferrero, R. Festa, L. Follia, G. Lettieri, S. Tarallo, T. Notari, A. Giarra, C. Marinaro, B. Pardini, A. Marano, G. Piaggeschi, C. Di Battista, M. Trifuoggi, M. Piscopo, L. Montano, A. Naccarati, Small noncoding RNAs and sperm nuclear basic proteins reflect the environmental impact on germ cells, Mol. Med. 30 (2024) 12, https://doi.org/10.1186/s10020-023-00776-6.
[47] A. Zhitkovich, Chromium in drinking water: sources, metabolism, and cancer risks, Chem. Res. Toxicol. 24 (2011) 1617–1629, https://doi.org/10.1021/tx200251t.
[48] J.D. Lewis, J. Ausió, Protamine-like proteins: evidence for a novel chromatin structure, Biochem. Cell. Biol. 80 (2002) 353–361, https://doi.org/10.1139/o02-083.
[49] J. Ausió, Histone H1 and evolution of sperm nuclear basic proteins, J. Biol. Chem. 274 (1999) 31115–31118, https://doi.org/10.1074/jbc.274.44.31115.
[50] F.M. Fioretti, F. Febbraio, A. Carbone, M. Branno, V. Carratore, L. Fucci, J. Ausió, M. Piscopo, A sperm nuclear basic protein from the sperm of the marine worm *Chaetopterus variopedatus* with sequence similarity to the arginine-rich C-termini of chordate protamine-likes, DNA Cell Biol. 31 (2012) 1392–1402, https://doi.org/10.1089/dna.2011.1547.
[51] M. Piscopo, M. Conte, F. Di Paola, S. Conforti, G. Rana, L. De Petrocellis, L. Fucci, G. Geraci, Relevance of arginines in the mode of binding of H1 histones to DNA, DNA Cell Biol. 29 (2010) 339–347, https://doi.org/10.1089/dna.2009.0993.
[52] J.M. Eirín-López, J.D. Lewis, L.A. Howe, J. Ausió, Common phylogenetic origin of protamine-like (PL) proteins and histone H1: evidence from bivalve PL genes, Mol. Biol. Evol. 23 (2006) 1304–1317, https://doi.org/10.1093/molbev/msk021.
[53] J.J. Phelan, J. Colom, C. Cozcolluela, J.A. Subirana, R.D. Cole, A lysine-rich protein from spermatozoa of the molluse *Mytilus edulis*, J. Biol. Chem. 249 (1974) 1099–1102, https://doi.org/10.1016/S0021-9258(19)42946-3.
[54] S. Carlos, L. Jutglar, I. Borrell, D.F. Hunt, J. Ausio, Sequence and characterization of a sperm-specific histone H1-like protein of *Mytilus californianus*, J. Biol. Chem. 268 (1993) 185–194.
[55] C. Rocchini, P. Rice, J. Ausio, Complete sequence and characterization of the major sperm nuclear basic protein from *Mytilus trossulus*, FEBS Lett. 363 (1995) 37–40, https://doi.org/10.1016/0014-5793(95)00275-e.
[56] M. Piscopo, M. Ricciardiello, G. Palumbo, J. Troisi, Selectivity of metal bioaccumulation and its relationship with glutathione S-transferase levels in gonadal and gill tissues of *Mytilus galloprovincialis* exposed to Ni (II), Cu (II) and Cd (II), Rend. Fis. Acc. Lincei 27 (2016) 737–748, https://doi.org/10.1007/s12210-016-0564-0.
[57] G. Lettieri, V. Mollo, A. Ambrosino, F. Caccavale, J. Troisi, F. Febbraio, M. Piscopo, Molecular effects of copper on the reproductive system of *Mytilus galloprovincialis*, Mol. Reprod. Dev. 86 (2019) 1357–1368, https://doi.org/10.1002/mrd.23114.
[58] A.B. Yılmaz, A. Yanar, E.N. Alkan, Review of heavy metal accumulation on aquatic environment in Northern East Mediterranean Sea part I: some essential metals, Rev. Environ. Health 32 (2017) 119–163, https://doi.org/10.1515/reveh-2016-0065.

[59] L. Rosati, T. Chianese, V. De Gregorio, M. Verderame, A. Raggio, C.M. Motta, R. Scudiero, Glyphosate interference in follicular organization in the wall lizard *Podarcis siculus*, Int. J. Mol. Sci. 24 (2023) 7363, https://doi.org/10.3390/ijms24087363.
[60] M. Verderame, T. Chianese, L. Rosati, R. Scudiero, Molecular and histological effects of glyphosate on testicular tissue of the lizard *Podarcis siculus*, Int. J. Mol. Sci. 23 (2022) 4850, https://doi.org/10.3390/ijms23094850.
[61] G. Lettieri, R. Notariale, N. Carusone, A. Giarra, M. Trifuoggi, C. Manna, M. Piscopo, New insights into alterations in PL proteins affecting their binding to DNA after exposure of *Mytilus galloprovincialis* to mercury—a possible risk to sperm chromatin structure? Int. J. Mol. Sci. 22 (2021) 5893, https://doi.org/10.3390/ijms22115893.
[62] R. Notariale, A. Basile, E. Montana, N.C. Romano, M.G. Cacciapuoti, F. Aliberti, R. Gesuele, F.D. Ruberto, S. Sorbo, G.C. Tenore, M. Guida, K.V. Good, J. Ausió, M. Piscopo, Protamine-like proteins have bactericidal activity. The first evidence in *Mytilus galloprovincialis*, Acta Biochim. Pol. 65 (2018) 585–594, https://doi.org/10.18388/abp.2018_2638.
[63] A.R. Bianchi, A. La Pietra, V. Guerretti, A. De Maio, T. Capriello, I. Ferrandino, Synthesis and degradation of poly(ADP-ribose) in zebrafish brain exposed to aluminum, Int. J. Mol. Sci. 24 (2023) 8766, https://doi.org/10.3390/ijms24108766.
[64] T.H. Vlahogianni, A. Valavanidis, Heavy-metal effects on lipid peroxidation and antioxidant defence enzymes in mussels *Mytilus galloprovincialis*, Chem. Ecol. 23 (2007) 361–371, https://doi.org/10.1080/02757540701653285.
[65] C. Marinaro, G. Lettieri, T. Chianese, A.R. Bianchi, A. Zarrelli, D. Palatucci, R. Scudiero, L. Rosati, A. De Maio, M. Piscopo, Exploring the molecular and toxicological mechanism associated with interactions between heavy metals and the reproductive system of *Mytilus galloprovincialis*, Comp. Biochem. Physiol. C Toxicol. Pharmacol. 275 (2024) 109778, https://doi.org/10.1016/j.cbpc.2023.109778.
[66] M. Piscopo, R. Notariale, F. Tortora, G. Lettieri, G. Palumbo, C. Manna, Novel insights into mercury effects on hemoglobin and membrane proteins in human erythrocytes, Molecules 25 (2020) 3278, https://doi.org/10.3390/molecules25143278.
[67] G. Carbone, G. Lettieri, C. Marinaro, M. Costabile, R. Notariale, A.R. Bianchi, A. De Maio, M. Piscopo, A molecular mechanism to explain the nickel-induced changes in protamine-like proteins and their DNA binding affecting sperm chromatin in *Mytilus galloprovincialis*: an in vitro study, Biomolecules 13 (2023) 520, https://doi.org/10.3390/biom13030520.
[68] D. Passaro, G. Rana, M. Piscopo, E. Viggiano, B. De Luca, L. Fucci, Epigenetic chromatin modifications in the cortical spreading depression, Brain Res. 1329 (2010) 1–9, https://doi.org/10.1016/j.brainres.2010.03.001.
[69] G. Lettieri, M. Maione, M.A. Ranauda, E. Mele, M. Piscopo, Molecular effects on spermatozoa of *Mytilus galloprovincialis* exposed to hyposaline conditions, Mol. Reprod. Dev. 86 (2019) 650–660, https://doi.org/10.1002/mrd.23141.
[70] V. De Guglielmo, R. Puoti, R. Notariale, V. Maresca, J. Ausió, J. Troisi, M. Verrillo, A. Basile, F. Febbraio, M. Piscopo, Alterations in the properties of sperm protamine-like II protein after exposure of *Mytilus galloprovincialis* (Lamarck 1819) to sub-toxic doses of cadmium, Ecotoxicol. Environ. Saf. 169 (2019) 600–606, https://doi.org/10.1016/j.ecoenv.2018.11.069.
[71] M. Prisco, M. Agnese, A. De Marino, P. Andreuccetti, L. Rosati, Spermatogenic cycle and steroidogenic control of spermatogenesis in *Mytilus galloprovincialis* collected in the bay of Naples, Anat. Rec. 300 (2017) 1881–1894, https://doi.org/10.1002/ar.23626.
[72] A. Chiarugi, M.A. Moskowitz, Cell biology. PARP-1–a perpetrator of apoptotic cell death? Science 297 (2002) 200–201, https://doi.org/10.1126/science.1074592.
[73] E. Prokhorova, F. Zobel, R. Smith, S. Zentout, I. Gibbs-Seymour, K. Schützenhofer, A. Peters, J. Groslambert, V. Zorzini, T. Agnew, J. Brognard, M.L. Nielsen, D. Ahel, S. Huet, M.J. Suskiewicz, I. Ahel, Serine-linked PARP1 auto-modification controls PARP inhibitor response, Nat. Commun. 12 (2021) 4055, https://doi.org/10.1038/s41467-021-24361-9.
[74] G. Guerriero, M.V. Brundo, S. Labar, A.R. Bianchi, S. Trocchia, D. Rabbito, G. Palumbo, F.K. Abdel-Gawad, A. De Maio, Frog (*Pelophylax bergeri*, Günther 1986) endocrine disruption assessment: characterization and role of skin poly (ADP-ribose) polymerases, Environ. Sci. Pollut. Res. Int. 25 (2018) 18303–18313, https://doi.org/10.1007/s11356-017-0395-2.
[75] L. Vitale, E. Vitale, G. Costanzo, A. De Maio, C. Arena, Photo-protective mechanisms and the role of poly (ADP-Ribose) polymerase activity in a facultative CAM plant exposed to long-term water deprivation, Plants 9 (2020) E1192, https://doi.org/10.3390/plants9091192.
[76] L. Vitale, E. Vitale, A.R. Bianchi, A. De Maio, C. Arena, Role of poly(ADP-ribose) polymerase (PARP) enzyme in the systemic acquired acclimation induced by light stress in *Phaseolus vulgaris L.* Plants, Plants 11 (2022) 1870, https://doi.org/10.3390/plants11141870.
[77] C. Arena, C. Mistretta, E. Di Natale, M.R.F. Mennella, A.V. De Santo, A. De Maio, Characterization and role of poly(ADP-ribosyl)ation in the Mediterranean species *Cistus incanus* L. under different temperature conditions, Plant Physiol. Biochem. 49 (2011) 435–440, https://doi.org/10.1016/j.plaphy.2011.02.004.
[78] Q.A. Vassalli, F. Caccavale, S. Avagnano, A. Murolo, G. Guerriero, L. Fucci, J. Ausió, M. Piscopo, New insights into protamine-like component organization in *Mytilus galloprovincialis*' sperm chromatin, DNA Cell Biol. 34 (2015) 162–169, https://doi.org/10.1089/dna.2014.2631.
[79] Z. Avramova, A. Zalensky, R. Tsanev, Biochemical and ultrastructural study of the sperm chromatin from *Mytilus galloprovincialis*, Exp. Cell Res. 152 (1984) 231–239, https://doi.org/10.1016/0014-4827(84)90248-9.
[80] A. Kinner, W. Wu, C. Staudt, G. Iliakis, Gamma-H2AX in recognition and signaling of DNA double-strand breaks in the context of chromatin, Nucleic Acids Res. 36 (2008) 5678–5694, https://doi.org/10.1093/nar/gkn550.
[81] E.H. Figueiredo Moura da Silva, L.A. Silva Antolin, A.J. Zanon, A. Soares Andrade, H. Antunes de Souza, K. dos Santos Carvalho, N. Aparecido Vieira, F.R. Marin, Impact assessment of soybean yield and water productivity in Brazil due to climate change, Eur. J. Agron. 129 (2021) 126329, https://doi.org/10.1016/j.eja.2021.126329.
[82] C. Grimm, C. Huntsberger, K. Markey, S. Inglis, R. Smolowitz, Identification of a Mycobacterium sp. as the causative agent of orange nodular lesions in the Atlantic sea scallop *Placopecten magellanicus*, Dis. Aquat. Org. 118 (2016) 247–258, https://doi.org/10.3354/dao02961.
[83] J. Zhao, B. Zhao, N. Kong, F. Li, J. Liu, L. Wang, L. Song, Increased abundances of potential pathogenic bacteria and expressions of inflammatory cytokines in the intestine of oyster *Crassostrea gigas* after high temperature stress, Dev. Comp. Immunol. 141 (2023) 104630, https://doi.org/10.1016/j.dci.2022.104630.
[84] T. Grune, T. Jung, K. Merker, K.J.A. Davies, Decreased proteolysis caused by protein aggregates, inclusion bodies, plaques, lipofuscin, ceroid, and "aggresomes" during oxidative stress, aging, and disease, Int. J. Biochem. Cell Biol. 36 (2004) 2519–2530, https://doi.org/10.1016/j.biocel.2004.04.020.
[85] C. Marinaro, G. Lettieri, M. Verrillo, M. Morelli, F. Carraturo, M. Guida, M. Piscopo, Possible molecular mechanisms underlying the decrease in the antibacterial activity of protamine-like proteins after exposure of *Mytilus galloprovincialis* to chromium and mercury, Int. J. Mol. Sci. 24 (2023) 9345, https://doi.org/10.3390/ijms24119345.